An Extended Control Strategy for Weakly Meshed Distribution Networks With Soft Open Points and Distributed Generation

DEJAN R. IVIC, (Member, IEEE), AND **PREDRAG C. STEFANOV**, (Member, IEEE)

School of Electrical Engineering, University of Belgrade, 11120 Belgrade, Serbia

Corresponding author: Dejan R. Ivic (id165006p@student.etf.bg.ac.rs)

ABSTRACT As part of the smart grid concept, different strategies specialized for power flow control in distribution networks have been developed. One of the possible solutions to optimize the utilization of existing capacities and increase distributed generation penetration is the implementation of Soft Open Points. Soft Open Points are modular devices based on power electronic converters that enable closing loops in the network without negative consequences regarding fault current propagation. Introducing the concept of soft open points in the distribution network enables power flow control in a particular part of the network and voltage control in the soft open point connecting nodes. The control strategy proposed in this paper addresses the main obstacle for appropriate exploitation of soft open points, defining reference values for control variables in the case of large-scale distribution systems. Furthermore, the proposed strategy also deals with data unavailability problems, that is, soft open point control under communication interruption. The proposed control algorithm incorporates centralized optimal power flow calculations and an estimation algorithm based on a multivariate polynomial regression. The optimal power flow is used to calculate the control variables in normal operation modes. The procedure based on multivariate polynomial regression was used to estimate the reference values of the control variables when the optimal power flow results were unavailable. This feature makes the proposed algorithm applicable to communication interruptions when only limited data capture is available. The algorithm proposed in this study was implemented and tested on a test network considering different scenarios. Conclusions and simulation results make this algorithm applicable to an actual soft open point controller.

INDEX TERMS Distribution automation, distributed generation integration, power flow control, soft open point, smart grid.

I. INTRODUCTION

Conventional medium-voltage distribution networks (with rated voltage range of 3 kV to 36 kV) are mainly characterized by a radial topology. To provide alternate supply and isolate faults, normally open points connecting adjacent feeders are integrated into the network [1]. Despite quite simple protection schemes, fast fault isolation, and supply restoration, this type of topology has some drawbacks related to the integration of distributed generators and controllable loads. These disadvantages mainly manifest as an uncontrollable load balance between feeders, peak currents, increased losses, and voltage excursions [2]. On the other hand, upgrading distribution networks to the looped configuration together with

The associate editor coordinating the review of this manuscript and approving it for publication was Youngjin Kim.

voltage profile improvement, load balance, and improved reliability brings a high risk of fault propagation. Closing the loops enables the fault current to propagate over a wider area and thus requires more complex and expensive protection schemes [3]. Soft Open Point (SOP) can be introduced as a compromise between two previously described concepts. Replacing normally open points with SOPs enables the combination of radial and meshed configuration benefits while avoiding the abovementioned drawbacks.

The integration of Distributed Energy Resources (DERs) into distribution networks brings many changes to the common control strategies of conventional distribution systems. The penetration of DERs causes reverse power flow in the distribution systems. Thus, the efficient and appropriate use of modern distribution networks with integrated DERs requires appropriate control algorithms. In addition to specially

developed control algorithms, hardware resources are required to establish the desired power flow control in the network. SOP can also be considered and used for this purpose.

The implementation of SOPs in power system operation and control purposes has already been presented in transmission networks as a back to back HVDC conversion system [4]. Improvements in power electronic devices, achieved in the past few decades, make this concept applicable to medium-voltage distribution networks (3–36 kV) [5]. The use of SOPs in distribution networks enables power flow control in a particular part of the network and ensures load balance between distribution feeders.

As the SOP realization is based on back-to-back converters, the reference values of the SOP' control variables are required for the appropriate and efficient application of SOPs. Many different algorithms for calculating the reference values of SOPs have been developed. Most of these algorithms are based on Optimal Power Flow (OPF) calculations [6], [7]. Their basis consists of an optimization framework that includes different SOP models, which are further introduced into the optimal power flow calculations. This type of algorithm considers an approach that requires many measurements within a network. The major challenge for such algorithms is data unavailability when OPF calculations cannot be performed for some reason. Data unavailability is mainly caused by different communication interruptions. In these cases, SOP control should be based on an alternative technique that enables the local control of the SOP. Different algorithms have been developed to ensure the SOP operation under communication interruptions. In [8], the algorithm for local control of the SOP is presented based on the voltage and power patterns. The algorithm designed to achieve local control of power flow through the SOP is described in [7] and [9]. This approach, which is also tested in a real 6 kV network, ensures voltage control in the connection nodes of the SOP, but does not analyze its influence on the rest of the network. A similar approach that enables local Volt/Var control was developed in [10]–[12]. These algorithms can be used during short communication interruptions as backup control strategies initialized when the OPF is unavailable.

The algorithm presented in the following chapters combines the OPF with an estimation-based control approach. When the OPF calculation results are not available, the developed algorithm calculates the SOP's control variables using a data history of few significant measurements located in particular network nodes. Each control variable can be estimated independently using the available data history set. This approach requires only basic mathematical operations, which makes it simple and easy to implement. Compared to the strategies above, designed for SOP operation under communication interruptions, the proposed algorithm ensures the operation of the entire distribution network using local control of the SOP. The applicability of the developed algorithm does not depend on the network topology or number of SOPs or DERs in the network.

The study presented in this paper contributes to the SOP control state of art in different ways. The most important contributions are summarized in two key points. First, an extended control framework for distribution networks with DGs covering the SOP operation under both normal and communication interruption conditions is formulated and clarified. Second, a completely novel algorithm for SOP operation under communication interruption was developed, implemented, and tested. The proposed algorithm is based on a polynomial-based estimation procedure, measurements available during communication interruption, and a data history set containing values measured over a specified period. Thus, the control strategy presented in this paper can easily be implemented in real cases, as a module of DMS or independently as a local SOP controller.

The remainder of this paper is organized as follows: The model of the SOP incorporated into the proposed control algorithm is described in detail in Section 2. Section 3 is dedicated to the optimization framework, which incorporates the SOP and treats it as a control resource in the network. The polynomial-based estimation procedure introduced to ensure the SOP operation during communication interruptions is described in Section 4. Section 5 presents case studies and the results of the simulations performed to test and validate the proposed control strategy. Finally, the conclusions and guidelines for further research are presented in the final section.

II. SOFT OPEN POINT MODEL

The main components of soft open point are power electronic converters, that is, configurations based on Voltage Source Converters (VSCs) [13]. The SOP connecting an arbitrary number (k) adjacent distribution feeders is illustrated in Fig. 1(a). The topology of the SOP composed of k VSCs is shown in Fig. 1(b). The main elements of this circuit are (i) VSCs based on insulated gate bipolar transistors (IGBTs), which are responsible for generating the desired voltage waveforms, and (ii) a DC capacitor, which ensures sufficient energy buffer and reduces DC voltage ripple. VSC terminals are further connected to the filter introduced to filter the high harmonics and limit the short-circuit current. The concept (SOP topology) presented in Fig.1 could be practically implemented as additional equipment to existing substations where distribution feeders are close to each other (for example, addition to Ring Main Units).

The described SOP architecture is adopted owing to the conveniences related to power/voltage control and fault isolation ability. The fully controllable active power flow is a consequence of the independent voltage waveforms of each VSC (waveforms produced using PWM). Simultaneously, independent voltage waveforms ensure independent reactive power injections (supply or absorption) at the SOP terminals [14]. Different control strategies can be used to achieve Volt/Var control [15], limit voltage transients and overcurrent, and ensure fault isolation. In this manner, using VSCs, faults on one feeder can be isolated from adjacent feeders. The selection of the aforementioned control strategy also depends

(a)

(b)
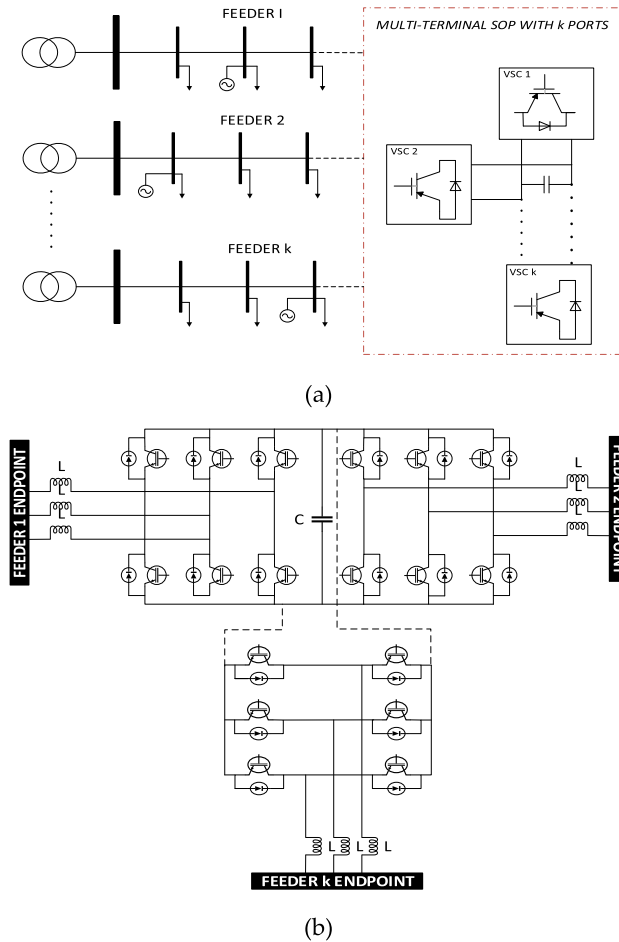
FIGURE 1. k-terminal SOP: (a) illustration; (b) Circuit topology.

on the SOP's operating mode. Different control strategies are implemented for the normal operating mode, fault isolation, and post-fault conditions (power supply restoration mode).

The proposed control algorithm was developed for normal operating mode. Thus, an appropriate control strategy based on the current control is used. This control strategy is also known as a dual closed-loop current-controlled strategy, as it contains two main loops (inner and outer loop) [16]. The three main parts of the current-controlled strategy are the outer control loop (power control), inner control loop (current control), and phase-locked loop (PLL). Compared to other control schemes used for VSC control (such as the voltage control scheme [17]–[19]), the current-controlled scheme ensures overcurrent protection, provides robustness against parameter variations, ensures better dynamic performance, and higher control precision [20]. These benefits make the current-controlled scheme widely applicable to different practical cases, which is also the reason for using such a strategy in this study. However, the main internal loops are only briefly stated to understand the importance and role of the reference values of the SOP outputs focused on in this study. Detailed mathematical relations that describe the internal SOP control loops can be found in [21]–[24].
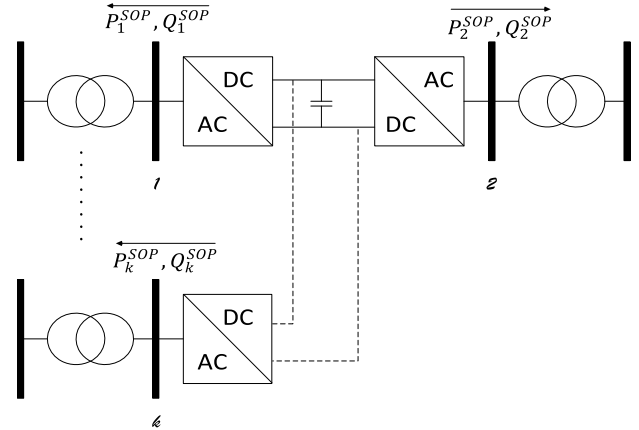
FIGURE 2. k-terminal SOP: power injection notations.

A. SOP MODEL IN POWER FLOW EQUATIONS

Considering the previously described control loops, a simplified block diagram of a multi-terminal SOP, which connects an arbitrary number (k) of AC nodes presented in Fig. 2, was adopted. According to the considerations presented in [25] and using the notation presented in Fig. 2, the active power flow through the SOP, which connects the k nodes in the network, is described using (1):

$$\sum_{h=1}^{k} \left(P_h^{SOP} + P_{h\,loss}^{SOP} \right) = 0, \tag{1}$$

where P_h^{SOP} denotes the active power injection from the SOP to the network (in node $h = 1, 2, \ldots k$) and P_{hloss} denotes active power losses in power electronic devices connected in node h. Owing to independent internal control loops for active/reactive power, DC voltage control, and SOP topology, reactive power injections in nodes $h = 1, 2, \ldots k$ (Q_h^{SOP}) are independent. The relation between active and reactive power injections from the SOP to the network is defined by the thermal limitations of power electronic devices (converters):

$$\sqrt{\left(P_h^{SOP} + P_{h\,loss}^{SOP} \right)^2 + \left(Q_h^{SOP} \right)^2} \le S_h^r; \tag{2}$$

where S_h^r denotes the apparent power of the VSC connected to nodes $h = 1, 2, \ldots, k$. Equations (1) and (2) describe the model of the multi-terminal SOP used in power flow calculations. These equations are also used to encompass the influence of the SOP on the network variables [26]. It should be noted that the active power losses in converters are included in this model. Accurate modeling of active power losses in VSCs requires an independent analysis that exceeds the scope of this study. For this reason, empirical models of losses obtained from a series of practical experiments are often used [15].

For the analysis and different simulations, simplified VSC loss estimations can also be introduced. Therefore, a simplified model of losses in the power electronic devices used in the proposed control algorithm is presented in the following paragraph.

B. SOFT OPEN POINT LOSSES ESTIMATION

The estimation of the active power losses in each converter of the SOP can be implemented using the model described by (3):

$$P_{converter}^{losses} = aI^2 + bI + c, \tag{3}$$

where I denotes the current through the converter leg (IGBT and diode, illustrated in Fig. 1 (b)), and a, b, and c are parameters of the switching components commonly provided by the manufacturers. Except for this model, the linearized model is often used as a sufficiently accurate approximation. A linearized model of losses in a power electronic converter can be represented as follows [27]:

$$P_{losses} = kI + c, \tag{4}$$

where

$$k = \left(P_{converter}^{losses\ rated} - c \right) / I_{rated}, \tag{5}$$

and c represents the converter losses independent of the load of the converter. Due to the relatively slight differences introduced by linearization, the linearized model of losses in power electronic converters is further used in the remainder of this paper.

In addition to losses in SOP switching components, additional losses caused by installation and environmental conditions (enclosure type, cable termination, etc.) could appear. In such cases, coefficients figuring in relation (3) and (4) should be slightly modified to encompass these additional heating losses. However, in most cases, losses in SOP switching components are much more dominant, so these additional losses are mostly neglected, as is the case in this study.

III. OPTIMIZATION-BASED OPERATION OF THE SOP

Under normal operating conditions, the operation of an SOP is based on the optimal power flow (OPF) calculations. Therefore, the optimization framework, defined to implement OPF in a distribution network with SOP, includes the following aspects: control variable definition, optimization criterion, optimization constraints, and criterion functions, that is, the mathematical expression of elements as mentioned above.

A. CONTROL VARIABLES DEFINITION

The control variable vector consists of active and reactive power injections in the direction adopted from the SOP to the network. The relations between the control variables are defined by the active power balance in the SOP and the thermal limitations of each converter used in the SOP. These relations, described by (1) and (2), respectively, must be fulfilled at any moment, and their implementation in the SOP control algorithm is mandatory.

With respect to the notation adopted in Fig. 2, in the case of the SOP connecting a total of k distribution feeders (SOP connecting k nodes in the network), the control variable

vector has $2k$-1 elements, and it is defined as:

$$x = \begin{bmatrix} P_1^{SOP} \\ \vdots \\ P_{k-1}^{SOP} \\ Q_1^{SOP} \\ \vdots \\ Q_k^{SOP} \end{bmatrix}. \tag{6}$$

In the case of an arbitrary number (N_{SOP}) of the SOPs in the network, the control variable vector, as defined above, is written for each of the SOPs in the network.

B. OPTIMIZATION CRITERIA

Different optimization criteria define different targets for the optimization procedure. The optimization criterion is used to rank all possible solutions that fulfill certain defined constraints. Two optimization criteria are commonly used in distribution networks: the minimal active power loss criterion and feeder load balance criterion. In the rest of the paper and all the simulations performed, the minimal active power loss criterion is considered. This choice does not affect the generality of the main conclusions or optimization framework design. Instead of this criterion, the load-balance criterion can be used. Additionally, a hybrid criterion can be defined by combining these two main criteria.

The minimal active power losses criterion is defined as:

$$\min \left(P_{loss}^{total} \right) = \min \left(P_{loss}^{network} + P_{losses}^{SOP} \right), \tag{7}$$

where both the network active power losses $P_{loss}^{network}$ and losses in the SOP converters P_{losses}^{SOP} are included.

C. OPTIMIZATION CONSTRAINTS

Optimal power flow (OPF) can be treated as a nonlinear multivariable constrained optimization procedure [28], [29]. Accordingly, constraints related to the network power flows and SOP thermal limits must be considered.

Network constraints are the consequence of distribution feeders/substations limits and active/reactive power balance in the network. Therefore, these equations can be classified into two types: equality-type and inequality-type. Active/reactive power balances define the equality-type network constraints. The power balance equations can be written using matrix notation as:

$$\left[P_{inj} \right] = [V] * \left([V]^T \times \left(G_{cos}^T + B_{sin}^T \right) \right)^T, \tag{8}$$

$$\left[Q_{inj} \right] = [V] * \left([V]^T \times \left(G_{sin}^T - B_{cos}^T \right) \right)^T, \tag{9}$$

where $*$ and $\times$ denote elementwise and matrix multiplication, respectively. The vectors and matrices introduced in the above relation are defined as follows, $\left[P_{inj} \right]$, $\left[Q_{inj} \right]$, $[G_{cos}]$, $[G_{sin}]$, $[B_{cos}]$, and $[B_{sin}]$, as shown at the bottom of the next page, where $i, j = 1, 2, 3, \ldots m$ denote network buses, P_i^G, Q_i^G denote active and reactive power generation connected to node i, P_i^L, Q_i^L denote active and reactive power consumption, and P_i^{SOP}, Q_i^{SOP} denote power injections from the SOP

connected to node i. Notations G_{ij}, B_{ij}, are real and imaginary parts of the admittance matrix element at position i,j, and $\theta_{ij} = \theta_i - \theta_j$ denotes the phase angle differences of voltages in nodes i and j. Equations (8) and (9) are the fundamentals of power flow calculations. The power balance described by these relations must be fulfilled at any moment.

Inequality-type network constraints can be described using equations (10) and (11):

$$I_{ij} \leq I_{ij}^{\max}, \tag{10}$$

$$V_i^{\min} \leq V_i \leq V_i^{\max}, \tag{11}$$

where $I_{ij}^{\max}$, $V_i^{\min}$, $V_i^{\max}$ denote the boundary values of network branch current and node voltages, respectively. Similar to the network constraints, the constraints of the SOP are classified into equality-type and inequality-type constraints. The equality-type constraints of the SOP are defined by the active power balance in the SOP described by relation (1). The inequality-type constraints of the SOP are related to the thermal limitations of the power electronic devices used for SOP implementation. These constraints are described by (2). The optimization framework presented in this chapter can be implemented using an arbitrary optimization method. It does not depend on the number of SOPs in the network or on the number of ports/terminals in each of the SOPs. The choice of the optimization method depends mainly on the desired performance and available computing resources. To avoid bothering this paper and considering the conclusions and models above, the simplest case of SOP with two ports is

considered in the rest of the paper and all simulations. This selection does not affect the applicability of the proposed control strategy or the conclusions described in the following sections. As could be noticed, all formulations presented in this section are suitable for three-phase balanced systems and, single-phase formulation is used. This choice comes from practical reasons. Despite many unbalanced distribution networks, symmetrical three-phase SOP realization is common in practical cases as their implementation is justified for economic and feasibility reasons. Furthermore, SOPs designed for unbalanced systems require additional expensive hardware, which will enable SOPs to act as active filters and ensure the symmetry of the considered network. Currently, large-capacity SOPs designed for unbalanced systems, which exceed the scope of this study, are not cost-effective, but they will be state-of-art in the near future.

The optimization methods and power flow calculation algorithms represent only the tools used to implement the proposed control strategy. Accordingly, their selection did not affect their applicability. The metaheuristic optimization method - Grey Wolf Optimizer (GWO), is used to implement a defined optimization framework. Except for metaheuristic methods [6], [11], [30], classical optimization methods have also been used [2], [31]. In this study, the metaheuristic optimization method was chosen to avoid constraint relaxation necessary to implement classical optimization methods [32]. At the same time, compared to other metaheuristic optimization algorithms, GWO retrieves results with good performance using minimal computing resources [33].

$$[P_{inj}] = \begin{bmatrix} P_1^G + P_1^{SOP} - P_1^L \\ P_2^G + P_2^{SOP} - P_2^L \\ \vdots \\ P_m^G + P_m^{SOP} - P_m^L \end{bmatrix}, \quad [Q_{inj}] = \begin{bmatrix} Q_1^G + Q_1^{SOP} - Q_1^L \\ Q_2^G + Q_2^{SOP} - Q_2^L \\ \vdots \\ Q_m^G + Q_m^{SOP} - Q_m^L \end{bmatrix},$$

$$[G_{\cos}] = \begin{bmatrix} G_{11} & G_{12}\cos(\theta_1 - \theta_2) & \cdots & G_{1m}\cos(\theta_1 - \theta_m) \\ G_{21}\cos(\theta_2 - \theta_1) & G_{22} & \cdots & G_{2m}\cos(\theta_2 - \theta_m) \\ \vdots & \vdots & \ddots & \vdots \\ G_{m1}\cos(\theta_m - \theta_1) & G_{m1}\cos(\theta_m - \theta_2) & \cdots & G_{mm} \end{bmatrix},$$

$$[G_{\sin}] = \begin{bmatrix} 0 & G_{12}\sin(\theta_1 - \theta_2) & \cdots & G_{1m}\sin(\theta_1 - \theta_m) \\ G_{21}\sin(\theta_2 - \theta_1) & 0 & \cdots & G_{2m}\sin(\theta_2 - \theta_m) \\ \vdots & \vdots & \ddots & \vdots \\ G_{m1}\sin(\theta_m - \theta_1) & G_{m2}\sin(\theta_m - \theta_2) & \cdots & 0 \end{bmatrix},$$

$$[B_{\cos}] = \begin{bmatrix} B_{11} & B_{12}\cos(\theta_1 - \theta_2) & \cdots & B_{1m}\cos(\theta_1 - \theta_m) \\ B_{21}\cos(\theta_2 - \theta_1) & B_{22} & \cdots & B_{2m}\cos(\theta_2 - \theta_m) \\ \vdots & \vdots & \ddots & \vdots \\ B_{m1}\cos(\theta_m - \theta_1) & B_{m2}\cos(\theta_m - \theta_2) & \cdots & B_{mm} \end{bmatrix},$$

$$[B_{\sin}] = \begin{bmatrix} 0 & B_{12}\sin(\theta_1 - \theta_2) & \cdots & B_{1m}\sin(\theta_1 - \theta_m) \\ B_{21}\sin(\theta_2 - \theta_1) & 0 & \cdots & B_{2m}\sin(\theta_2 - \theta_m) \\ \vdots & \vdots & \ddots & \vdots \\ B_{m1}\sin(\theta_m - \theta_1) & B_{m2}\sin(\theta_m - \theta_2) & \cdots & 0 \end{bmatrix},$$

IV. THE POLYNOMIAL-BASED ESTIMATION ALGORITHM–SOP OPERATION UNDER COMMUNICATION INTERRUPTIONS

The SOP control could be implemented locally during the unavailability of OPF caused by communication interruption or any other failure in the DMS operation. This local control is based on measurements available during interruptions and a polynomial-based estimation procedure. The estimation procedure, used to achieve local control of SOP during communication interruptions, consists of three main subsequences: forming a training data set, training procedure (i.e., calculating polynomial coefficients), and polynomial-based estimation procedure.

A. THE TRAINING DATA SET

Before the estimation procedure is implemented, an appropriate training data set must be formed. For example, to train the control algorithm to encompass states of data unavailability, the training data set should be formed to contain the appropriate history of data obtained by the OPF in a defined period.

For this purpose, the following procedure for forming the training data set can be used:

- Perform OPF calculations during periods of normal operating modes of the SOP. The OPF calculation procedure considers the SOP as a control resource in the network.
- Store the OPF data (i.e., SOP output values, active/ reactive power load/generation) for a while before the moment of communication interruption– for example, 24 h before the considered moment of interruption (with hourly sampling rate);
- Classify stored values and prepare them for further use in the estimation procedure. This step encompasses sorting, filtering, and storing the data in the most suitable manner to be quickly extracted during the estimation procedure.

The complete procedure described above was based on the power flow calculations. The network variables that make the training data set could be measured values during periods of the regular operation of the SOP or eventually estimated values in some specific virtual measurements. The training data set also has to contain the weather information related to the capturing period (cloudy period or clear-sky period) to encompass the variations in PV plant production. This information could be later introduced to predict the expected estimation accuracy, define some predefined estimation sequences, and improve the estimation performance.

B. POLYNOMIAL COEFFICIENT CALCULATION - MULTIVARIATE POLYNOMIAL REGRESSION

The optimization framework presented in the previous section enables the calculation of the SOP control variables using OPF. In cases of communication interruptions or cases in which OPF results are not available for any other reason,

the estimation of the SOP control variables could be used. For this purpose, different estimation procedures are used. Estimation based on artificial neural networks and predictive control specialized for HVDC control [35], [36] can be adjusted and used to control the SOP. In addition, specialized control strategies based on fuzzy logic for distribution networks with power electronic devices presented in [37] can also be introduced. All the estimation strategies stated above require a data history set for training/prediction. The data history set contains the measured values of the particular voltages and currents/powers within the network. Commonly, a data history set is formed using the data retrieved from all available metering points within the network. These values were further sorted, filtered, and processed to represent the network history in a defined period.

With the exception of polynomial regression, used in the proposed approach, some related regression techniques such as Autoregressive Moving Average (ARMA), Autoregressive Integrated Moving Average (ARIMA), or Autoregressive Moving Average with exogenous terms (ARMAX) could also be considered. More details related to these estimation techniques can be found in [38]–[40]. Compared to polynomial regression, all the models mentioned above are classified as linear signal models.

During communication interruptions, the current values of some measurements within the network remain available through remaining/alternate communication channels or by manual input. Accordingly, polynomial estimation based on these values seems to be the most suitable technique for estimating the necessary SOP reference values. Owing to the possibility of adjusting coefficients and the degree of variables in multivariate polynomials, polynomial-based estimation is expected to track changes in the control variables and, simultaneously, to ensure high estimation accuracy. Linear, single-variable estimation, as the simplest form of polynomial estimation, cannot estimate rapid changes in the control variables. Therefore, this case of polynomial estimation must be neglected.

Following the previously defined model of the SOP and considering the estimation targets, it can be concluded that all control variables of the SOP are independently estimated. Thus, each control variable of the SOP is considered as a single-output static system governed by the m variable smooth function:

$$y = g(x_1, x_2, x_3, \ldots, x_{am}). \qquad (12)$$

In (12), y represents the control variable of the SOP (active and reactive power injections from the SOP to the network), and $x_1, x_2, \ldots, x_{am}$ are independent variables that determine the system behavior. In the considered case, these variables are some of the available network variables (node voltages and/or branch currents/power flows) archived together with the SOP output values in the training data history set. Therefore, the relation (12) can be approximated using the

p-th order polynomial described in [41]:

$$\Pi_p = \beta_0 + \sum_{l_1=1}^{am} \beta_{l_1} x_{l_1} + \sum_{l_1=1}^{am} \sum_{l_2=l_1}^{am} \beta_{l_1 l_2} x_{l_1} x_{l_2} + \cdots$$

$$+ \sum_{l_1=1}^{am} \sum_{l_2=l_1}^{am} \cdots \sum_{l_p=l_{p-1}}^{am} \beta_{l_1 l_2 \cdots l_p} x_{l_1} x_{l_2} \cdots x_{l_p}, \quad (13)$$

where p is a non-negative integer, and β_0, β_1, $\beta_{l1\ l2}$, ..., $\beta_{l1\ l2,...lp}$ are polynomial coefficients. The multivariable function (13) is linear with respect to the polynomial coefficients, implying that Least Square Estimator (LSE) can be used.

In the case of the existing data history of N OPF calculations, that is, y_i $(i = 1, 2, \ldots, N)$ values of the SOP control variable and $x_{i1}, x_{i2}, \ldots, x_{iam}$ values of independent (input) variables from the training data set, considering x_{l1}, $x_{l2}, \ldots, x_{lj}$ $(j = 1, 2, 3 \ldots)$ multivariable function Π_p can be represented in vector form as follows:

$$Y = \Phi\Theta + E, \quad (14)$$

where $Y = \begin{bmatrix} y_1 & y_2 & \cdots & y_N \end{bmatrix}^T$ is a vector of results (considered SOP control variable calculated by OPF), $\Theta = \begin{bmatrix} \beta_0 & \beta_1 & \cdots & \beta_{am} & \cdots & \beta_{11\cdots11} & \beta_{11\cdots12} \cdots & \beta_{amam\cdots am} \end{bmatrix}^T$ is the parameter vector, and $E = \begin{bmatrix} \varepsilon_1 & \varepsilon_2 & \cdots & \varepsilon_N \end{bmatrix}^T$ is an error vector. Φ denotes the loading matrix, which can be expressed as:

$$\Phi = \begin{bmatrix} 1 & x_{11} & \cdots & x_{1am} & \cdots & x_{11}^p & x_{11}^{p-1}x_{12} & \cdots & x_{1am}^p \\ 1 & x_{21} & \cdots & x_{2am} & \cdots & x_{21}^p & x_{21}^{p-1}x_{22} & \cdots & x_{2am}^p \\ \vdots & \vdots & \vdots & \vdots & \vdots & \vdots & \vdots & \vdots & \vdots \\ 1 & x_{N1} & \cdots & x_{Nam} & \cdots & x_{N1}^p & x_{N1}^{p-1}x_{N2} & \cdots & x_{Nam}^p \end{bmatrix}.$$

In cases where the matrix $\Phi^T\Phi$ is invertible, the LSE can be used to estimate the polynomial coefficients:

$$\Theta^* = (\Phi^T\Phi)^{-1}\Phi^T Y. \quad (15)$$

In the case of large dimensions of matrix Φ, QR factorization can be used to avoid explicit matrix inversion [41]. In cases where matrix $\Phi^T\Phi$ is not invertible, the truncated Least Square estimation [42], [43] can be used to estimate the polynomial parameters.

C. ESTIMATION OF SOP's OUTPUTS DURING COMMUNICATION INTERRUPTION

After calculating the polynomial coefficients, all the preconditions necessary to calculate the SOP outputs were fulfilled. The outputs of the SOP during communication interruptions can be calculated as:

$$y^{|*} = g(x_1, x_2, x_3, \ldots, x_{am}). \quad (16)$$

where y^* denotes the SOP output, and $x_1, x_2, \ldots, x_{am}$ are network variables (available measurements) captured after communication interruption has occurred. Function g is a polynomial function described by the coefficients calculated using (15). Similar to the training data set, the available measurement set contains weather information (clear or cloudy sky), so the expected estimation accuracy range could be calculated.
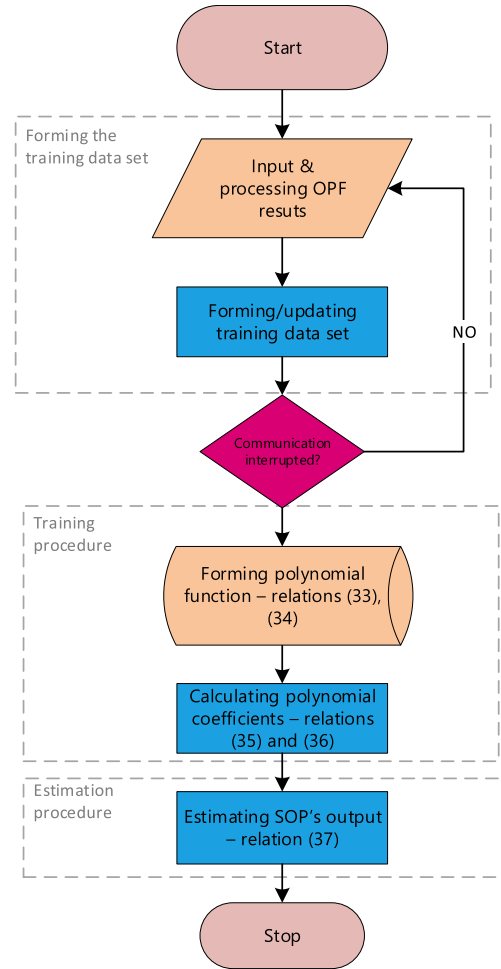
FIGURE 3. The polynomial-based estimation algorithm flowchart.

By introducing the polynomial coefficients Θ^* estimated using relation (15), the resulting polynomial function (Π_p^*) can be used to calculate the control variables of the SOP for any new value of the considered independent (network) variables. A flowchart of the polynomial-based estimation procedure is presented in Fig. 3.

The implementation of the previously described procedure on training data sets and available measurements makes a local control algorithm that requires only basic math operations – multiplication and summation. The main obstacle during implementation could be the decision to choose appropriate network variables. As this decision depends on a few factors such as the SOP's location, the capacity of loads in the network, network topology, current configuration, etc., the choice of appropriate variables cannot be generalized. It can only be defined by analyzing the correlation between particular measured values in the network and using operator experience and simulation results.

V. CASE STUDIES
A. TEST SYSTEM
To test the proposed algorithm, an SOP control strategy was implemented and simulated in the IEEE 33 test network. The detailed network parameters are presented in [36].

To analyze the impact of DERs, a photovoltaic power plant with a rated power of 5 MW located at node 10 of the test system was considered. The SOP location and network configuration are adopted, as shown in Fig. 4. The particular choice of the number and location of the SOPs selected to present the proposed control strategy does not affect the final conclusions.

Distributed generators integrated into the test network are considered to operate in the P-Q operating mode. They are modeled as power injections in the connecting bus and are further treated as negative loads [44]. The power electronic converter parameters employed correspond to the actual devices obtained from different vendors. The rated apparent power of the converters was 3 MVA.

Loads in the network are modeled as an aggregated load connected to the network nodes and classified into several groups: residential loads (groups D1-D3), commercial loads (group K), and industrial loads (group I). Normalized load diagrams for each load group, together with the production diagram of the PV plant, are presented in Fig. 5. In power flow calculations, the load-voltage dependence was modeled using the ZIP model. The production diagram of the PV plant, presented in Fig. 5, is based on the incident solar radiation measured at the location with geographic coordinates of 44.7866° N and 20.4489° E (Belgrade, Serbia).

As the data set necessary for the control algorithm "training," the results obtained by OPF based on Grey Wolf Optimizer are used. For each load/generator, the load/production was varied up to 5% during the considered period relative to the baseline diagrams presented in Fig. 5. A power flow algorithm based on the impedance matrix [45] was introduced as a power-flow calculation tool. SOP active power losses, presented in Section 2, were directly introduced to the power flow calculation algorithm, and such calculated values were further introduced in the OPF and estimation procedures.

The boundary values of the current, representing the thermal constraints of the power lines, were adopted for each line in the network. For simulation purposes, an overload of any line in the network was not considered. Boundary values of voltages in the network buses are defined as: $V_{\min} = 0.9$ p.u. and $V_{\max} = 1.05$ p.u. The operation of the network without an SOP was analyzed as a benchmark for comparison. Simulations implemented to validate the proposed control strategy encompass different scenarios based on different training and testing data sets. Different scenarios are structured and described in the following paragraphs, depending on key factors related to the DER, that is, PV plant production.

B. CASE STUDY 1

The first case study encompasses a scenario in which training and testing data sets are defined based on similar periods of PV plant production, that is, either clear or cloudy periods. The estimation procedure was performed considering the measurements (network variables), as listed in Table 1.

In addition to the choice of network variables, their degree in the estimated polynomial significantly affects the
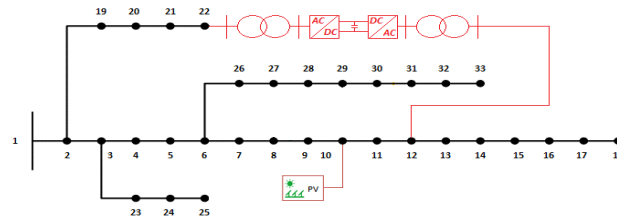
FIGURE 4. IEEE 33 test network with added SOP.

TABLE 1. Set of available network variables case study 1.

Network variable	Notation in polynomial	Description
P_{24}	x_1	Three of the most dominant active power loads in the network.
P_{25}	x_2	
P_{32}	x_3	
Q_{30}	x_4	Three of the most dominant reactive power loads in the network.
Q_{24}	x_5	
Q_{32}	x_6	
P_{DG10}	x_7	Active power generation from the distributed generator – PV plant located in node 10

estimation quality. Therefore, all possible polynomial forms should be considered to achieve high-quality estimation. The degree of each network variable in the resulting polynomial defines the number of coefficients that must be calculated. This value is also limited by the available data history set used to perform the estimation.

For simulation purposes, the data history set was limited to 24h. The degree of each network variable in the resulting polynomial form is limited to ≤ 3. The Root Mean Square Error (RMSE) was used as a tool to compare different polynomials. According to the simulation results, to achieve the most accurate estimation, each SOP output was estimated using different polynomial forms. These differences are represented by network variables and degree levels in the resulting polynomial. The estimated SOP outputs can be represented as:

$$P_l^{SOP}$$
$$= f(x_1, x_2, x_7) = a_7 x_7 + a_2 x_2 + a_{27} x_2 x_7 + a_1 x_1$$
$$+ a_{17} x_1 x_7 + a_{12} x_1 x_2 + a_{127} x_1 x_2 x_7 + a_{11} x_1^2 + a_{117} x_1^2 x_7$$
$$+ a_{112} x_1^2 x_2 + a_{10} + a_{111} x_1^3; \qquad (17)$$

$$Q_l^{SOP}$$
$$= f(x_4, x_5, x_6) = b_6 x_6 + b_{66} x_6^2 + b_5 x_5$$
$$+ b_{56} x_5 x_6 + b_{566} x_5 x_6^2 + b_{55} x_5^2 + b_{556} x_5^2 x_6$$
$$+ b_4 x_4 + b_{46} x_4 x_6 + b_{466} x_4 x_6^2 + b_{45} x_4 x_5$$
$$+ b_{456} x_4 x_5 x_6 + b_{455} x_4 x_5^2 + b_0 + b_{555} x_5^3; \qquad (18)$$

$$Q_m^{SOP}$$
$$= f(x_2, x_4, x_5, x_6, x_7) = c_7 x_7 + c_6 x_6 + c_{67} x_6 x_7 + c_5 x_5$$
$$+ c_{57} x_5 x_7 + c_{56} x_5 x_6 + c_4 x_4 + c_{47} x_4 x_7 + c_{46} x_4 x_6$$
$$+ c_{26} x_2 x_6 + c_{25} x_2 x_5 + c_{24} x_2 x_4$$
$$+ c_0 + c_{22} x_2^2 + c_{44} x_4^2 + c_{55} x_5^2; \qquad (19)$$

where $a_0, \ldots a_{111}, b_0, \ldots b_{555}, c_0, \ldots c_{55}$ are real coefficients calculated by performing a polyfit-based algorithm for each of the SOP outputs independently. These coefficients are updated with time, as different moments of communication
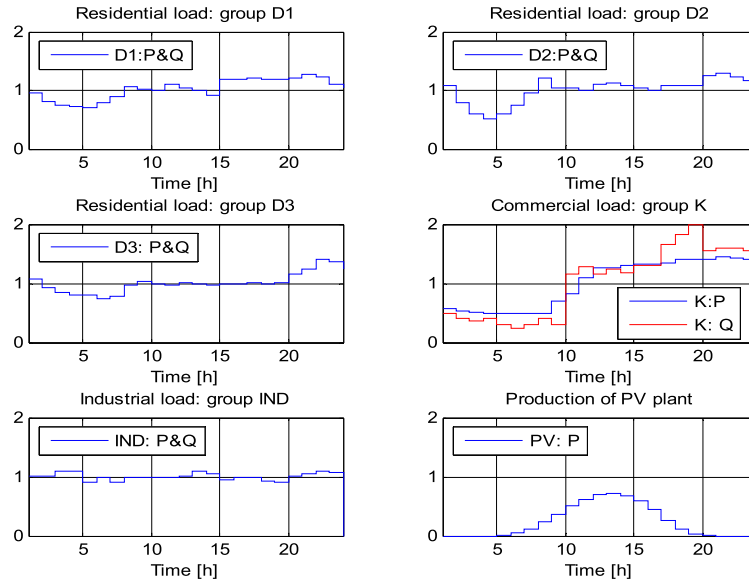
FIGURE 5. Load/Production diagrams.
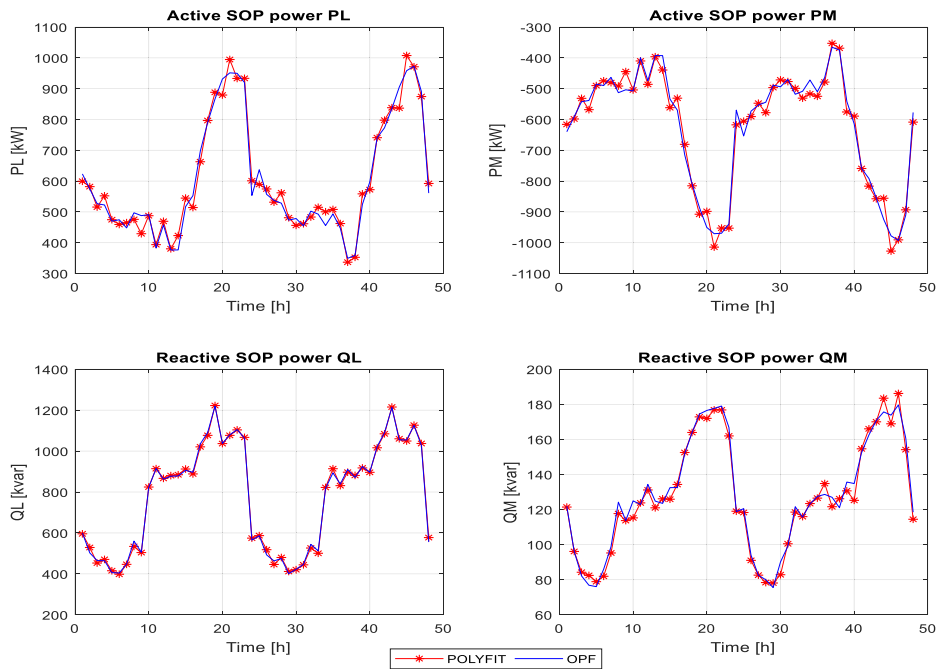
FIGURE 6. SOP output variables–case study 1.

interruption are considered, that is, for each of the considered 48 h. A graphical interpretation of the estimated SOP outputs during the considered simulation period together with the appropriate OPF values is presented in Fig. 6. From Fig. 6, it can be concluded that the estimated output variables of the SOP are very close to the corresponding values obtained by the OPF.

The total active power losses in the network for the first case study for 48 h are presented in Table 2 and Fig. 7.

The analysis of the simulation results presented in Table 2 and Fig. 7 can be summarized as follows:

– Total active power loss minimization is the most efficient when the SOP operates using the OPF results, that is, when there is no communication interruption. In contrast, maximum active power losses occur in the base case when the SOP is completely turned off.

– The active power loss reduction obtained using the SOP control variables estimation, based on polynomial regression, is very close to the active power loss reduction obtained using the OPF.

– Active power loss minimization, performed using SOP control variables estimation based on polynomial

TABLE 2. Total active power losses–case study 1.

Time [h]	Total network Ploss [kW]				Time [h]	Total network Ploss [kW]			
	Without SOP	SOP fixed	OPF	PolyFIT		Without SOP	SOP fixed	OPF	PolyFIT
1	129.89	93.29	93.28	93.32	25	132.52	95.83	95.45	95.58
2	106.99	78.71	78.16	78.19	26	101.85	75.58	74.67	74.71
3	92.68	68.52	68.40	68.41	27	94.58	69.95	69.80	69.81
4	89.73	65.84	65.84	65.89	28	91.68	67.05	67.04	67.11
5	76.56	57.97	57.72	57.72	29	76.69	58.14	57.86	57.87
6	79.04	60.05	60.05	60.14	30	80.77	60.98	60.96	60.96
7	81.56	63.12	62.72	62.78	31	83.13	64.40	64.03	64.06
8	106.40	85.73	80.70	80.77	32	105.44	85.03	80.04	80.09
9	108.28	99.88	85.63	85.68	33	106.47	97.37	83.14	83.22
10	155.92	162.76	117.09	117.16	34	147.59	155.10	110.94	110.98
11	174.97	214.41	136.04	136.27	35	180.22	225.39	136.88	136.95
12	172.45	262.75	133.35	133.45	36	167.42	264.91	130.43	130.83
13	173.85	289.06	137.87	137.96	37	179.11	281.19	141.95	141.96
14	164.89	292.56	128.68	128.89	38	166.72	286.40	131.89	131.96
15	192.76	330.90	147.29	147.44	39	195.44	325.15	148.15	148.94
16	198.61	277.58	151.63	151.84	40	204.48	293.09	154.10	155.07
17	255.66	263.06	186.43	186.55	41	257.11	270.65	184.54	184.92
18	291.93	233.23	207.87	207.94	42	284.72	226.47	202.55	202.57
19	350.22	251.80	245.23	245.24	43	336.70	241.26	235.96	235.98
20	314.02	219.76	217.78	217.94	44	306.57	213.62	212.05	212.33
21	331.60	229.13	229.00	229.11	45	329.11	227.98	227.93	228.08
22	339.70	235.27	235.22	235.23	46	354.71	245.29	245.24	245.24
23	318.93	221.99	221.84	221.85	47	300.28	209.97	209.56	209.58
24	124.16	109.03	94.21	94.34	48	125.41	110.08	95.35	95.42

regression, gives the best results when it is most needed, during periods when the PV plant injects the most power into the network. This feature is directly driven by introducing the values of the PV plant power injection in the estimation procedure. Compared to the case when the SOP is completely turned off during communication interruptions, the total active power losses during peak hours of PV production (10-18h) could be decreased by 24.44% by operating the SOP using control variable estimation.

For comparison, Fig. 7 also shows the active power losses in the case where the SOP uses the last known set points (OPF values just before the communication interruption), that is, the SOP operation with fixed outputs. As expected, fixed SOP outputs cannot track changes caused by power injection from the PV plant, thus, polynomial-based estimations are a better solution in such cases.

C. CASE STUDY 2
Considering the variations in PV plant production based on weather variation, significant differences between the

training and testing data sets could occur. These differences are most noticeable in the following scenarios:

- Scenario 1: When the training data set contains data captured during periods of clear sky and estimation of SOP outputs should be performed during cloudy periods.
- Scenario 2: When the estimation shall be implemented during clear sky periods and training data set contains data captured during cloudy periods.

Both of the scenarios stated above encompass the case of a significant difference between PV plant outputs in the training and testing data sets. Similar to the first case study, the data history set was limited to 24h, and the degree of each network variable in the resulting polynomial form is limited to ≤3. Again, the RMSE was used to compare the estimations based on different polynomial forms. The SOP outputs when the training procedure is performed during cloudy periods and estimation is performed during clear-sky periods are presented in Fig. 8.

Compared to the estimation results from the first case study, the estimation of the SOP outputs, in this case, is slightly different, especially when considering the reactive
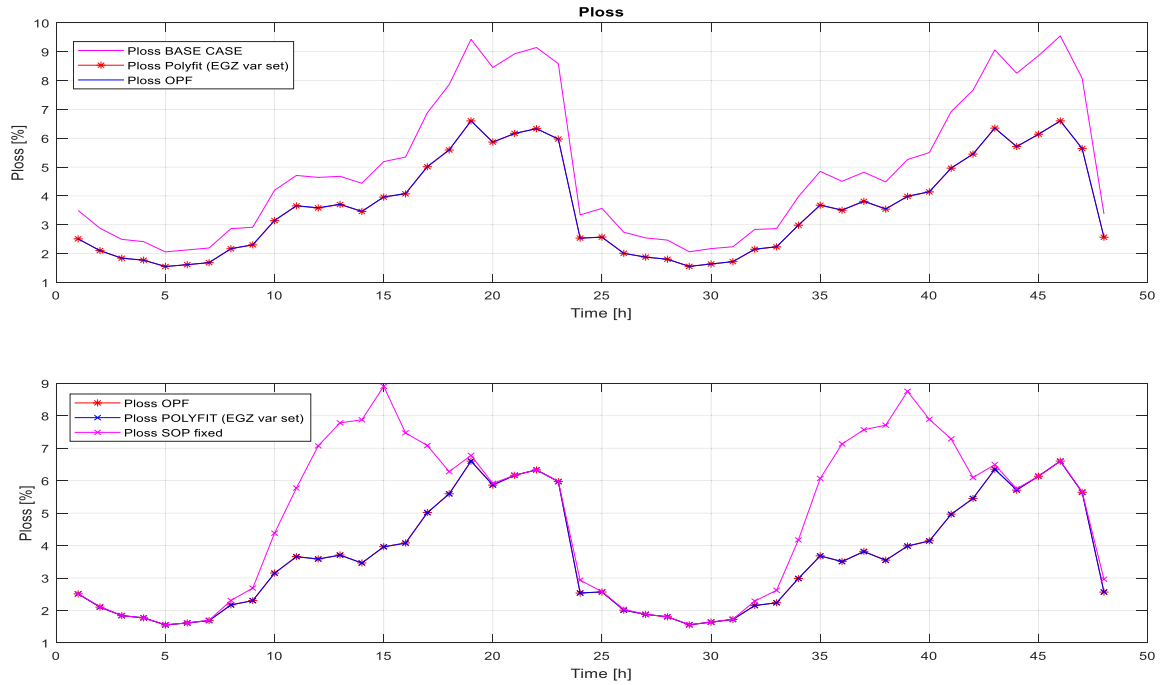
FIGURE 7. Simulation results: total active power losses–case study 1.
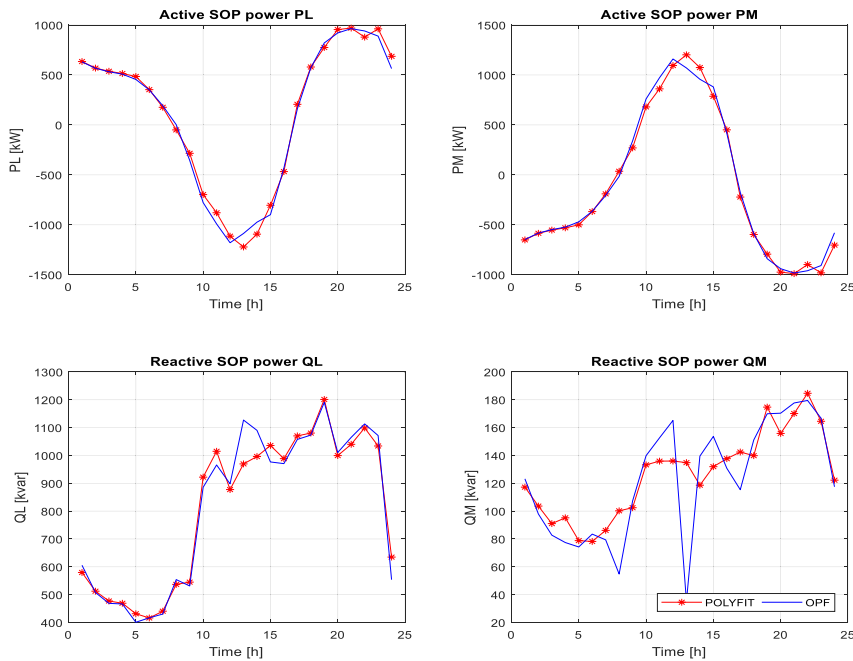
FIGURE 8. SOP output variables–case study 2, scenario 1.

powers of the SOP. These differences could be interpreted as a direct consequence of the difference between the PV outputs in the training and testing data sets. As the PV output (and its influence on network variables) is significantly larger in testing than in the training data set, the estimation procedure is less accurate compared to the scenario analyzed in case study 1.

The second scenario tested in this case study encompasses cloudy periods as a testing data set and periods of clear sky included in the training data set. The SOP outputs estimated with respect to this scenario are shown in Fig. 9. Considering the simulation results presented in Fig. 9, it can be concluded that in this scenario, the estimation algorithm provides better accuracy considering both active and reactive
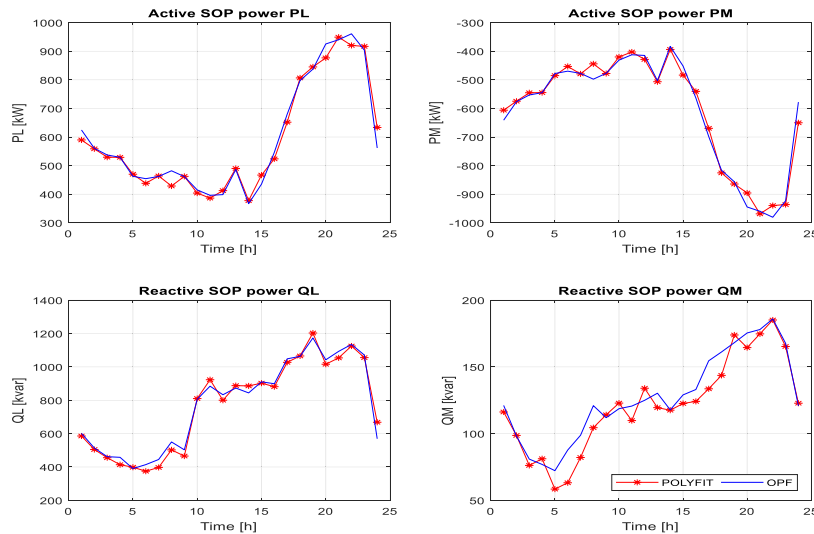
FIGURE 9. SOP output variables–case study 2, scenario 2.

power injections of the SOP. Furthermore, as the PV output is larger in the training data set than in the testing data set, the algorithm tackles the output peaks much better than in the previous scenario.

Further estimation improvements in both scenarios analyzed above could be achieved by introducing an additional solar irradiance parameter into the estimation procedure. In this manner, the most suitable training data set could be selected so that the training data capture includes the period with irradiance values near to the value captured or estimated during communication interruption.

In both scenarios analyzed above, the algorithm ensures an accurate estimation of the active power injections of the SOP. Simultaneously, the active power injections of the SOP significantly affected the total active power losses in the network. Thus, the total active power losses in the network obtained using the SOP output estimation in both scenarios are very close to the values obtained using the OPF calculations. For example, the total active power losses in the network calculated for Scenario two are presented in Fig. 10.

Graphs presented in Fig. 10 could also be used to compare the efficiency of the proposed polynomial-based estimation algorithm to the simplest estimation procedure - linear estimation. According to the results presented in Fig. 10, the benefits of polynomial-based estimation over linear estimation could easily be quantified. It shows up that linear estimation is not suitable to track changes in SOP outputs, or even worse, linear estimation in some cases leads to increased active power losses compared to the defined benchmark (case without SOP).

D. EFFICACY AND PERFORMANCE INDICES
The study of the efficacy and performance of the proposed control algorithm was conducted as an additional subsequence of the case studies presented above.

The algorithm efficacy is investigated using a defined optimization criterion, that is, total active power losses in the network. Similar to the paragraphs above, total active power losses in the network are compared between two cases of SOP operation: OPF-based operation and operation based on the proposed estimation algorithm. The maximal relative error between the power losses in these two cases of SOP operation was used as a index of the algorithm efficacy. The efficacy indices of the proposed algorithm, for all scenarios described above, are presented in Table 3.

TABLE 3. Algorithm efficacy parameters.

	Case study 1	Case study 2 Scenario 1	Case study 2 Scenario 3
Maximal relative error [%]	0.2322	0.6583	3.0613

The values presented in Table 3 indicate satisfactory accuracy level of the polynomial-based estimation algorithm in all the analyzed scenarios. As expected, the lowest accuracy of the proposed estimation algorithm is in the scenario when estimation is implemented for clear-sky periods and the training data set contains values captured during cloudy sky. However, the accuracy achieved in this scenario (value of relative error below 5%) is more than satisfactory for the practical implementation of the proposed control algorithm.

Besides accuracy, the processing time is a very important parameter for the implementation of the proposed algorithm. The total processing time necessary to implement the proposed estimation algorithm can be divided into training and calculation times. As stated in Section 4 and presented in the above case studies, the algorithm performance depends on the polynomial degree. This value affects the estimation of the SOP value and the necessary length of the data history set.
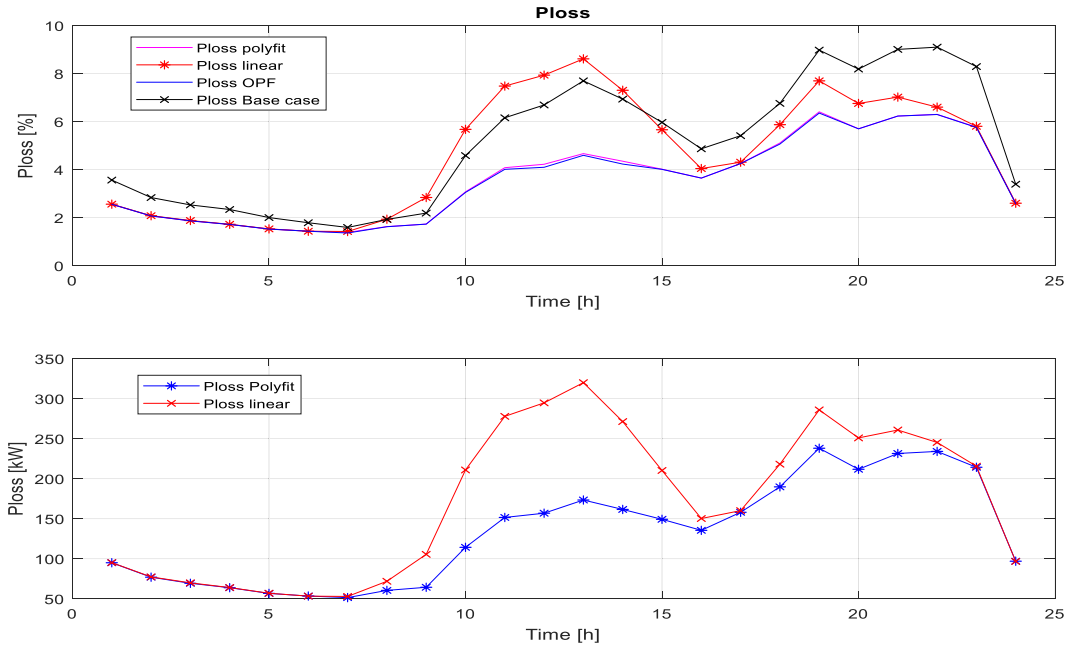
FIGURE 10. Total active power losses in the network–case study 2, scenario 2.
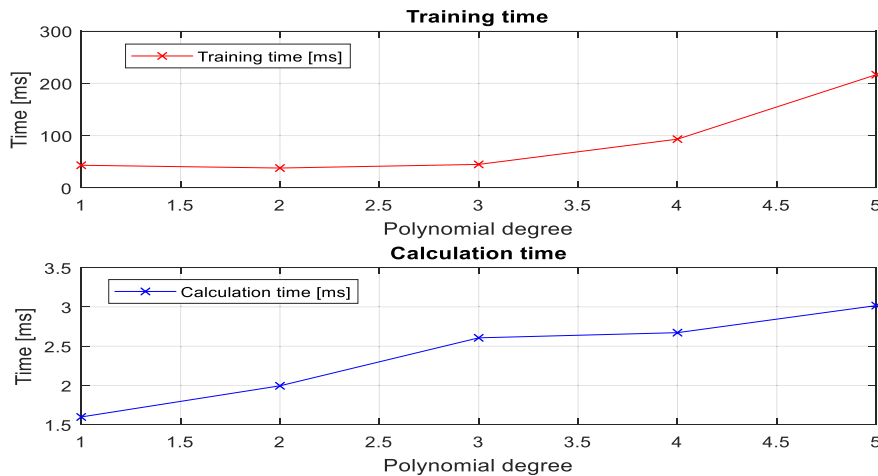
FIGURE 11. Algorithm processing time for different values of polynomial degree (single SOP output).

The training and calculation times of a single SOP output estimation for different polynomial degree values are presented in Fig. 11. From Fig. 11, it is evident that the calculation time, necessary for the estimation of a single SOP output, fits into a couple of milliseconds while appropriate training time fits into a range from 50 to 250 milliseconds. These values are significant for the applicability of the proposed algorithm. As the proposed SOP control strategy is designed for real-time implementation, the values presented in Fig. 11 indicate the applicability of the proposed algorithm to real SOP controllers. It should be emphasized that all simulations were performed using a regular PC (i5-7300U CPU, 8GB RAM). In real cases, the computational resources (server machines) are much better, so the values presented in Fig.11 are expected to be significantly lower.

E. DEMONSTRATION OF APPLICABILITY AND ROBUSTNESS

The benefits of SOPs are most noticeable in large networks. On the other hand, the implementation of SOPs in large networks requires a more complex communication infrastructure for the transmission of larger data sets. Consequently, larger networks are more susceptible to potential communication interruptions. The proposed control strategy is designed as an effective tool to ensure the continuous operation of SOPs in such large-scale systems.

To demonstrate the applicability of the proposed algorithm and test its robustness in large-scale networks, a modified IEEE 69 buses test network is analyzed. A single-line diagram of this system is presented in Fig. 12. The basic (radial) configuration is changed by adding 2 SOPs and 3 DER.
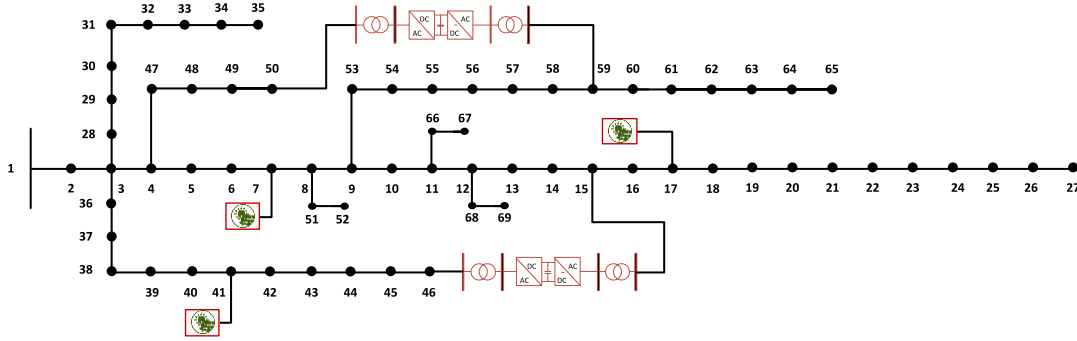
FIGURE 12. IEEE 69 network with SOPs and DERs added.
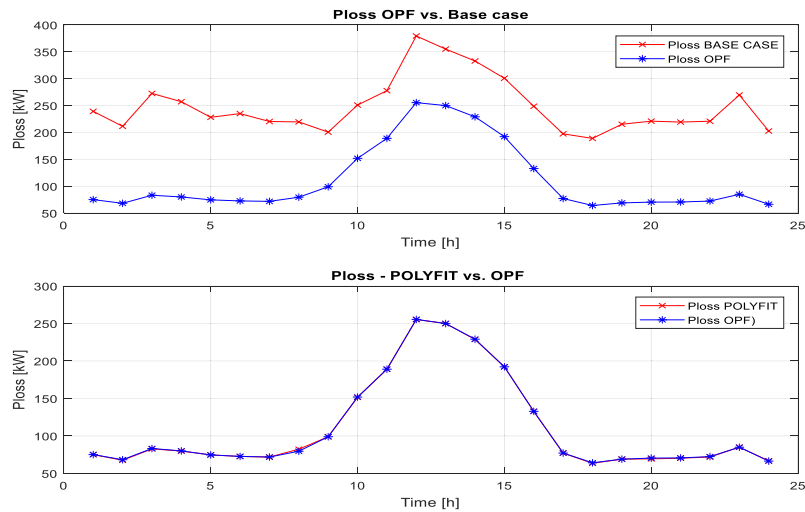
FIGURE 13. Total active power losses in the network–modified IEEE 69 test network.
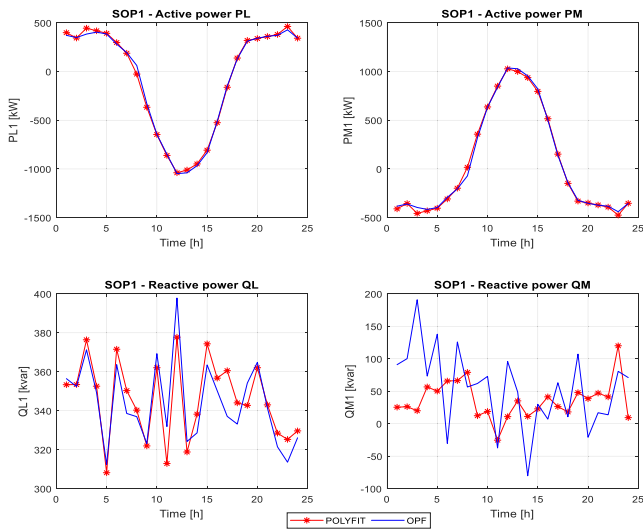
FIGURE 14. SOP1 Output estimation modified IEEE 69 test network.
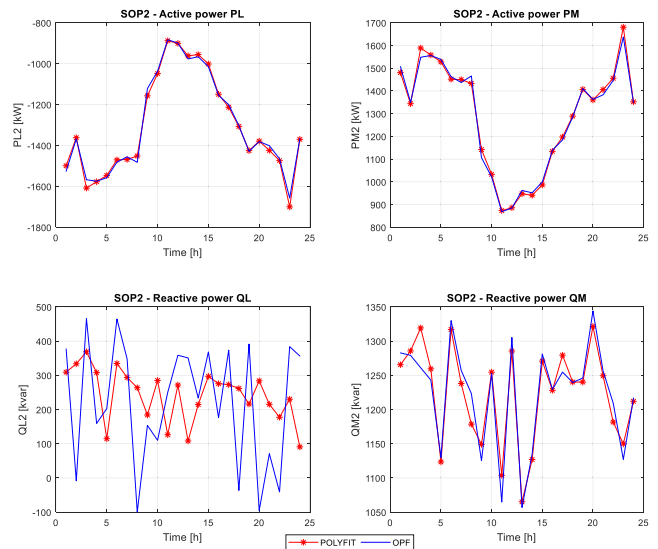
FIGURE 15. SOP2 Output estimation modified IEEE 69 test network.

Network loads and generation from DER are modeled as already described in Section 5.1. All other simulation parameters, such as the length of the data history data set, the limit values of the polynomial degrees were also similar to those

in 5.1. As expected, a larger network with multiple SOPs and DERs required a larger set of available measurements necessary to ensure the efficient operation of the proposed control algorithm. The set of available measurements used

in this case study is presented in Table 4. Simulations were performed for all scenarios presented in 5.2. The simulation results for the most expected scenario (similar radiation in the data sets for training and testing) are shown in Fig. 13. Estimated outputs of the SOPs are presented in Fig. 14 and Fig. 15.

As can be seen from Fig. 13, the proposed control algorithm shows good performance in the case of a larger network with an increased number of SOPs and DERs integrated into the network. Even in the worst case, when both SOPs operate using a polynomial-based estimation algorithm, the total active power losses in the network are very close to the values obtained during the operation of the OPF-based SOP. The above simulation results once again confirm the wide range of applicability of the proposed algorithm. The applicability of the proposed control strategy does not depend directly on the number of SOPs and DERs in the network.

VI. CONCLUSION

Introducing Soft Open Points (SOPs) into a conventional medium-voltage distribution network brings significant benefits related to the increased efficiency and operating flexibility of the considered network. These benefits are the most visible in networks with a high penetration of renewable energy resources (distributed generators), where SOPs play an important role in power flow control and efficient utilization of available capacities in the network. On the other hand, efficient operation of the SOP requires the development of appropriate control strategies designed to ensure the operation of the SOP under normal operating conditions as well as in cases where communication interruptions occur.

The control strategy presented in this paper encompasses both normal operation modes when the OPF is used to calculate the SOP control variables and operation under communication interruption when the SOP control variables are estimated using a polynomial-based estimation procedure. In this manner, the SOP is continuously operating, so turning the SOP off during communication interruptions is completely avoided.

The results of simulations performed in the analyzed case studies could serve as representative efficiency indicators of the implemented control strategy. Compared to the base case, without SOP in the network, or compared to the cases when SOP outputs are frozen during communication interruptions, the implemented control strategy significantly decreases the total active power losses in the network, compensates load peaks in the network, and releases existing capacities to enable an increase in distributed generator penetration.

The necessity of data history can be identified as a shortcoming of the proposed control strategy. The data set, consisting of measured values of currents, voltages, and load/generation, is often unavailable in existing conventional distribution networks. In this case, implementing the proposed control strategy requires the first acquisition of the necessary data set by introducing appropriate metering

points, which will be used as a basis for the polynomial estimation of SOP outputs. On the other hand, the simplicity of implementation combined with good performance is the main advantage of the control strategy analyzed in this study. The proposed control strategy requires a metaheuristic optimization method to perform OPF under normal operating conditions and applies only basic mathematical operations to estimate the optimal SOP outputs during periods when OPF is unavailable. As the proposed control strategy does not depend on the dimensions of the network, the number of SOPs in the network, and the number of distributed generators integrated into the network, it is applicable to a wide range of existing (real) distribution networks.

The main contribution of this study is the complete control framework covering normal and operating conditions with communication problems. Furthermore, the presented control strategy and appropriate simulation results are the basis for further research in this area. As has already been emphasized, the choice of network variables plays a crucial role in the estimation procedure. It has also been stated that the desired estimation performance can be achieved using different polynomial forms, depending on the limitations related to the number of introduced network variables and polynomial degrees. These topics will be within the scope of the author's future research focused on improving the estimation performance and reducing the necessary data set.

REFERENCES

[1] A. J. Momoh, *Electric Power Distribution, Automation, Protection, and Control*. Boca Raton, FL, USA: CRC Press, 2007.

[2] C. Wang, G. Song, P. Li, H. Ji, J. Zhao, and J. Wu, "Optimal configuration of soft open point for active distribution network based on mixed-integer second-order cone programming," in *Proc. Appl. Energy Symp. Forum*, Apr. 2016, pp. 70–75.

[3] M. A. Abdullah, A. P. Agalgaonkar, and K. M. Muttaqi, "Assessment of energy supply and continuity of service in distribution network with renewable distributed generation," *Appl. Energy*, vol. 113, pp. 1015–1026, Jan. 2014.

[4] K. V. Sood, *HVDC and Facts Controllers*. New York, NY, USA: Springer, 2004.

[5] J. M. Guerrero, P. C. Loh, T.-L. Lee, and M. Chandorkar, "Advanced control architectures for intelligent microgrids—Part II: Power quality, energy storage, and AC/DC microgrids," *IEEE Trans. Ind. Electron.*, vol. 60, no. 4, pp. 1263–1270, Apr. 2013.

[6] J. Flottemesch and M. Rother, "Optimized energy exchange in primary distribution networks with DC links," in *Proc. IEEE Int. Conf. Electr. Utility Deregulation, Restructuring Power Technol.*, Hong Kong, Apr. 2004, pp. 108–116.

[7] N. Okada, "A method to determine the distributed control setting of looping devices for active distribution systems," in *Proc. IEEE Bucharest PowerTech.*, Bucharest, Romania, Dec. 2009, pp. 1–6, doi: 10.1109/PTC.2009.5281982.

[8] A. Marano-Marcolini, M. B. Villarejo, A. Fragkioudaki, J. M. Maza-Ortega, E. Ramos, A. de la Villa Jaen, and C. C. Delgado, "DC link operation in smart distribution systems with communication interruptions," *IEEE Trans. Smart Grid*, vol. 7, no. 6, pp. 2962–2970, Nov. 2016, doi: 10.1109/TSG.2016.2589544.

[9] N. Okada, "Verification of control method for a loop distribution system using loop power flow controller," in *Proc. IEEE PES Power Syst. Conf. Expo.*, Atlanta, GA, USA, Apr. 2006, pp. 2116–2123, doi: 10.1109/PSCE.2006.296271.

[10] H. Hafezi and H. Laaksonen, "Autonomous soft open point control for active distribution network voltage level management," in *Proc. IEEE Milan PowerTech.*, Milan, Italy, Oct. 2019, pp. 1–6, doi: 10.1109/PTC.2019.8810735.

[11] P. Li, H. Ji, and H. Yu, "Combined decentralized and local voltage control strategy of soft open points in active distribution networks," *Appl. Energy*, vol. 241, pp. 613–624, Oct. 2019, doi: 10.1016/j.apenergy.2019.03.031.

[12] Q. Hou, J. Zheng, and N. Dai, "Application of soft open point for flexible interconnection of urban distribution network," in *Proc. IEEE PES Asia–Pacific Power Energy Eng. Conf. (APPEEC)*, Macao, China, Oct. 2019, pp. 1–5, doi: 10.1109/APPEEC45492.2019.8994697.

[13] J. M. Bloemink and T. C. Green, "Benefits of distribution-level power electronics for supporting distributed generation growth," *IEEE Trans. Power Del.*, vol. 28, no. 2, pp. 911–919, Apr. 2013.

[14] W. Yazdani and R. Iravani, *Voltage-sourced Converters in Power Systems*. Hoboken, NJ, USA: Wiley, 2010.

[15] S. Cole, J. Beerten, and R. Belmans, "Generalized dynamic VSC MTDC model for power system stability studies," *IEEE Trans. Power Syst.*, vol. 25, no. 3, pp. 1655–1662, Aug. 2010.

[16] C. L. Trujillo, D. Velasco, J. G. Guarnizo, and N. Díaz, "Design and implementation of a VSC for interconnection with power grids, using the method of identification the system through state space for the calculation of controllers," *Appl. Energy*, vol. 88, no. 9, pp. 3169–3175, Sep. 2011.

[17] N. R. Chaudhuri, R. Majumder, B. Chaudhuri, and J. Pan, "Stability analysis of VSC MTDC grids connected to multimachine AC systems," *IEEE Trans. Power Del.*, vol. 26, no. 4, pp. 2774–2784, Oct. 2011.

[18] J. M. Espi Huerta, J. Castello-Moreno, J. R. Fischer, and R. Garcia-Gil, "A synchronous reference frame robust predictive current control for three-phase grid-connected inverters," *IEEE Trans. Ind. Electron.*, vol. 57, no. 3, pp. 954–962, Mar. 2010.

[19] I. J. Balaguer, Q. Lei, S. Yang, U. Supatti, and F. Z. Peng, "Control for grid-connected and intentional islanding operations of distributed power generation," *IEEE Trans. Ind. Electron.*, vol. 58, no. 1, pp. 147–157, Jan. 2011.

[20] L. G. B. Rolim, D. R. da Costa, and M. Aredes, "Analysis and software implementation of a robust synchronizing PLL circuit based on the pq theory," *IEEE Trans. Ind. Electron.*, vol. 53, no. 6, pp. 1919–1926, Dec. 2006.

[21] E. Romero-Ramos, A. Marano-Marcolini, and J. Maza-Ortega, "Assessing the loadability of active distribution networks in the presence of DC controllable links," *IET Gener., Transmiss. Distrib.*, vol. 5, no. 11, pp. 1105–1113, Nov. 2011.

[22] W. R. Erickson and D. Maksimovic, *Fundamentals of Power Electronics*. New York, NY, USA: Springer, 2001.

[23] D. Van Hertem, J. Verboomen, R. Belmans, and W. L. Kling, "Power flow controlling devices: An overview of their working principles and their application range," in *Proc. Int. Conf. Future Power Syst.*, Amsterdam, The Netherlands, 2005, pp. 16–18.

[24] F. Belloni, R. Chiumeo, C. Gandolfi, and M. Brenna, "Application of back-to-back converters in closed-loop and meshed MV distribution grid," in *Proc. AEIT Annu. Conf. From Res. Ind.*, Sep. 2014, pp. 1–6.

[25] W. Cao, J. Wu, N. Jenkins, C. Wang, and T. Green, "Operating principle of soft open points for electrical distribution network operation," *Appl. Energy*, vol. 164, pp. 245–257, Feb. 2016.

[26] D. Sciano, A. Raza, R. Salcedo, M. Diaz-Aguilo, R. E. Uosef, D. Czarkowski, and F. de Leon, "Evaluation of DC links on dense-load urban distribution networks," *IEEE Trans. Power Del.*, vol. 31, no. 3, pp. 1317–1326, Jun. 2016.

[27] B. Dokic and B. Blanusa, *Power Electronics*. Cham, Switzerland: Springer 2015.

[28] K. Bhattacharya, "Optimization principles: Practical applications to the operation and markets of the electric power industry," *IEEE Power Energy Mag.*, vol. 3, no. 6, pp. 75–76, Nov. 2005.

[29] R. Simanjorang, Y. Miura, T. Ise, S. Sugimoto, and H. Fujita, "Application of series type BTB converter for minimizing circulating current and balancing power transformers in loop distribution lines," in *Proc. Power Convers. Conf.*, Nagoya, Japan, Apr. 2007, pp. 997–1004.

[30] Q. Qi, J. Wu, and C. Long, "Multi-objective operation optimization of an electrical distribution network with soft open point," *Appl. Energy*, vol. 208, pp. 734–744, Dec. 2017.

[31] C. Long, J. Wu, L. Thomas, and N. Jenkins, "Optimal operation of soft open points in medium voltage electrical distribution networks with distributed generation," *Appl. Energy*, vol. 184, pp. 427–437, Dec. 2016.

[32] H. Ji, C. Wang, P. Li, J. Zhao, G. Song, and J. Wu, "Quantified flexibility evaluation of soft open points to improve distributed generator penetration in active distribution networks based on difference-of-convex programming," *Appl. Energy*, vol. 218, pp. 338–348, May 2018.

[33] E. Cuevas, E. B. Espejo, and A. C. Enriquez, *Metaheuristics Algorithms in Power Systems*. Cham, Switzerland: Springer 2019.

[34] S. Mirjalili, S. M. Mirjalili, and A. Lewis, "Grey wolf optimizer," *Adv. Eng. Softw.*, vol. 69, pp. 46–61, Mar. 2014.

[35] S. Li, M. Fairbank, C. Johnson, D. C. Wunsch, E. Alonso, and J. L. Proao, "Artificial neural networks for control of a grid-connected rectifier/inverter under disturbance, dynamic and power converter switching conditions," *IEEE Trans. Neural Netw. Learn. Syst.*, vol. 25, no. 4, pp. 738–750, Apr. 2014.

[36] S. Mariethoz, A. Fuchs, and M. Morari, "A VSC-HVDC decentralized model predictive control scheme for fast power tracking," *IEEE Trans. Power Del.*, vol. 29, no. 1, pp. 462–471, Feb. 2014.

[37] A. Luo, C. Tang, Z. Shuai, J. Tang, X. Yong Xu, and D. Chen, "Fuzzy-PI-based direct-output-voltage control strategy for the STATCOM used in utility distribution systems," *IEEE Trans. Ind. Electron.*, vol. 56, no. 7, pp. 2401–2411, Jul. 2009.

[38] D. C. Montgomery, E. A. Peck, and G. G. Vining, *Introduction to Linear Regression Analysis*. Hoboken, NJ, USA: Wiley, 2012.

[39] H. Gatignon, *Statistical Analysis of Management Data*, Norwell, MA, USA: Kluwer, 2003.

[40] P. Campagnoli, S. Petrone, and G. Petris, *Dynamic Linear Models With R*. New York, NY, USA: Springer-Verlag, 2009.

[41] W. D. Scott, *Multivariate Density Estimation*. Hoboken, NJ, USA: Wiley, 2015.

[42] T. F. Chan and P. C. Hansen, "Some applications of the rank revealing QR factorization," *SIAM J. Sci. Stat. Comput.*, vol. 13, no. 3, pp. 727–741, May 1992.

[43] R. D. Fierro, G. H. Golub, P. C. Hansen, and D. P. O' Leary, "Regularization by truncated least squares," *SIAM J. Sci. Comput.*, vol. 18, no. 4, pp. 1223–1241, Jul. 1997.

[44] D. Shirmohammadi, H. W. Hong, A. Semlyen, and G. X. Luo, "A compensation-based power flow method for weakly meshed distribution and transmission networks," *IEEE Trans. Power Syst.*, vol. 3, no. 2, pp. 753–762, May 1988.

[45] P. Stefanov, "Weakly meshed distribution networks with distributed generation—Power flow analysis using improved impedance matrix based algorithm," in *Proc. Int. Symp. Ind. Electron.*, Banja Luka, Bosnia, Nov. 2016, pp. 1–6.

DEJAN R. IVIC (Member, IEEE) received the B.Sc. degree in electric power systems from the Faculty of Electrical Engineering, University of Banja Luka, Bosnia and Herzegovina, in 2015, and the M.Sc. degree in electric power systems and networks from the School of Electrical Engineering, University of Belgrade, Belgrade, Serbia, in 2016, where he is currently pursuing the Ph.D. degree in electric power systems and networks. His interests include power system operation optimization, power systems automation and control (especially distribution automation), and implementation of power electronics in power systems.

PREDRAG C. STEFANOV (Member, IEEE) received the B.Sc., M.Sc., and Ph.D. degrees in electrical engineering from the School of Electrical Engineering, University of Belgrade, Belgrade, Serbia, in 1988, 1995, and 2004, respectively. He is currently an Associate Professor with the Department of Electrical Power Systems, School of Electrical Engineering, University of Belgrade.

• • •